Dalton
www.rsc.org/dalton

O,N-Coordinated *o*-iminobenzoquinone and *o*-iminobenzosemiquinonato(1−) ligands in complexes of Ni(II), Co(III) and Fe(III)

Kil Sik Min, Thomas Weyhermüller and Karl Wieghardt *
Max-Planck-Institut für Strahlenchemie, Stiftstrasse 34-36, D-45470 Mülheim an der Ruhr, Germany

Received 25th November 2002, Accepted 29th January 2003
First published as an Advance Article on the web 12th February 2003

Octahedral complexes of the type $[M(tren)(L^{IBQ})]^{n+}$ or $[M(tren)(L^{ISQ})]^{n+}$ (tren = tris(2-aminoethyl)amine; L^{IBQ} = *o*-iminobenzoquinone, $(L^{ISQ})^{1-}$ = *o*-iminobenzosemiquinonate(1−) π radical, M = Ni, Co, Fe) have been prepared by the reaction of equimolar amounts of 2-anilino-4,6-di-*tert*-butylphenol, tris(2-aminoethyl)amine, $M(CH_3CO_2)_2\cdot 4H_2O$ (M = Ni, Co) or $FeCl_2\cdot 4H_2O$ in CH_3OH containing 2 equivalents of NEt_3 and air. The following complexes were isolated and characterized by X-ray crystallography: red–black $[Ni^{II}(tren)(L^{IBQ})](PF_6)_2$ (**1**), green $[Ni^{II}(tren)(L^{ISQ})](ClO_4)$ (**2**), brown $[Co^{III}(tren)(L^{ISQ})](ClO_4)_2\cdot 0.5CH_3OH\cdot 0.5H_2O$ (**3**), $[Fe^{III}(tren)(L^{ISQ})](ClO_4)_2\cdot 0.5CH_3OH\cdot 0.5H_2O$ (**4**). Their electrochemistry has been studied and the oxidized and reduced species have been characterized by UV-vis, EPR and Mössbauer spectroscopy. Temperature-dependent magnetic susceptibility measurements (2–290 K) reveal that **1** possesses an $S = 1$, **2** an $S = 3/2$, **3** an $S = ½$, and **4** an $S = 0$ ground state. The metrical details of *O,N*-coordinated $(L^{AP}\text{-H})^{2-}$, $(L^{ISQ})^{1-\bullet}$, and $(L^{IBQ})^{0}$ ligands are clearly established. $(L^{AP}\text{-H})^{2-}$ represents the aromatic dianion *o*-iminophenolate.

Introduction

It is now well established[1–8] that *O,N*-coordinated *o*-aminophenolate ligands are redox non-innocent in the sense that they can be bound to a transition metal ion either as an *o*-imidophenolate dianion, $(L^{AP}\text{-H})^{2-}$, or as an *o*-iminobenzosemiquinonate π radical monoanion, $(L^{ISQ})^{1-\bullet}$, or as an *o*-aminophenolate monoanion $(L^{AP})^{1-}$. In principle, the *o*-iminobenzoquinone, $(L^{IBQ})^{0}$, level of oxidation is also conceivable but to date it has been discovered electrochemically[2,3] in solution only. Thus, in contrast to a recent claim[9a] no complex containing an *O,N*-coordinated *o*-iminobenzoquinone ligand has been structurally characterized with the exception of a copper(I) species containing an *O,N*-coordinated 2,4,6,8-tetra-*tert*-butylphenoxazin-1-one ligand.[9b] In Scheme 1 the established structural differences between an *O,N*-coordinated $(L^{AP}\text{-H})^{2-}$ and an $(L^{ISQ})^{1-\bullet}$ are summarized[6] where the ligand is always derived from 2-anilino-4,6-di-*tert*-butylphenol, $H[L^{AP}]$. Upon one-electron oxidation of aromatic $(L^{AP}\text{-H})^{2-}$ to the radical anion $(L^{ISQ})^{1-\bullet}$ the C–O and C–N bond distances of the *o*-aminophenolate ring decrease by ~0.04 Å. The C–C distances of this ring are nearly equidistant in $(L^{AP}\text{-H})^{2-}$ but display a quinoid-type distortion in $(L^{ISQ})^{1-}$. It is expected that this trend is further amplified upon oxidation to the $(L^{IBQ})^{0}$ level as has been structurally verified for many *o*-benzosemiquinonate and *o*-benzoquinone transition metal ion complexes.[10,11]

We have synthesized a series of octahedral complexes containing the M(tren)-fragment and an *O,N*-coordinated $(L^{ISQ})^{1-}$ or (L^{IBQ}) ligand: $[Ni^{II}(tren)(L^{IBQ})](PF_6)_2$ (**1**), $[Ni^{II}(tren)(L^{ISQ})](ClO_4)$ (**2**), $[Co^{III}(tren)(L^{ISQ})](ClO_4)_2\cdot 0.5CH_3OH\cdot 0.5H_2O$ (**3**) and $[Fe^{III}(tren)(L^{ISQ})](ClO_4)_2\cdot 0.5CH_3OH\cdot 0.5H_2O$ (**4**). Here, tren represents the tetradentate ligand tris(2-aminoethyl)amine.

Three similar complexes have been reported previously with 3,5-di-*tert*-butylcatecholate[12] or 3,6-di-*tert*-butylcatecholate[13] ligands or their benzosemiquinonate(1−) radical anions: $[Co^{III}(tren)(3,5\text{-DTCat})]^{+}$, $[Cr^{III}(tren)(3,6\text{-DTCat})]^{+}$, and $[Cr^{III}(tren)(3,6\text{-DTBSQ})]^{2+}$.

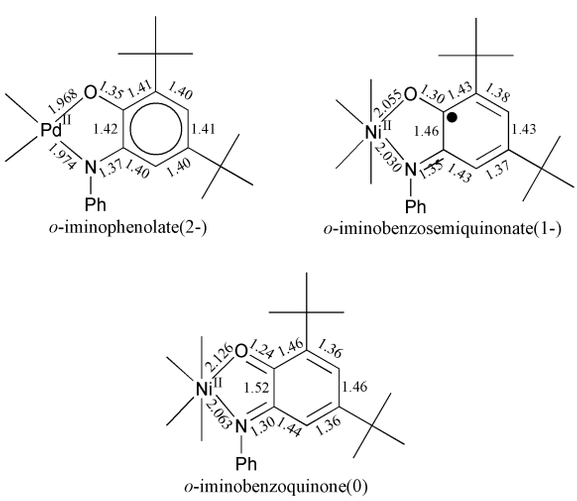

o-iminophenolate(2-) *o*-iminobenzosemiquinonate(1-) *o*-iminobenzoquinone(0)

Scheme 1

Experimental

Materials

The ligand 2-anilino-4,6-di-*tert*-butylphenol, $H[L^{AP}]$, has been prepared as described in the literature.[2]

Syntheses

$[Ni(tren)(L^{IBQ})](PF_6)_2$ (1). To a solution of $Ni(CH_3CO_2)_2\cdot 4H_2O$ (0.25 g, 1.0 mmol) in MeOH (10 mL) was added with stirring a methanol solution (5 mL) of tris(2-aminoethyl)amine (0.15 g, 1.0 mmol), solid $H[L^{AP}]$ (0.30 g, 1.0 mmol), and triethylamine (0.28 mL, 2.0 mmol) at room temperature. The mixture was stirred for about 30 min after which time a methanol solution (10 mL) of $LiPF_6$ (0.90 g) was added. The solution was oxidized by the passage of a stream of air through the solution for 2 h. During the oxidation a red–black microcrystalline precipitate formed which was filtered off, washed with cold MeOH, and dried in air. Yield: 0.40 g (51%). Electrospray ionization mass spectrometry (ESI-MS): *m/z* (CH_2Cl_2) = 644 $[(M - PF_6)^{+}$, 20%], 249 $[(M - 2PF_6)^{2+}$, 100%]. Anal. Calc. for $C_{26}H_{43}F_{12}N_5NiOP_2$: C, 39.52; H, 5.48; N, 8.86. Found: C, 39.45; H, 5.45; N, 8.78%.

$[Ni(tren)(L^{ISQ})]ClO_4$ (2). To a solution of $Ni(CH_3CO_2)_2\cdot 4H_2O$ (0.25 g, 1.0 mmol) in MeOH (10 mL) was added with

DOI: 10.1039/b211698g

Table 1 Crystallographic data for **1**, **2**, **3**·0.5MeOH·0.5H_2O, **4**·0.5MeOH·0.5H_2O

	1	**2**	**3**·0.5MeOH·0.5H_2O	**4**·0.5MeOH·0.5H_2O
Formula	$C_{26}H_{43}F_{12}N_5NiOP_2$	$C_{26}H_{43}BF_4N_5NiO$	$C_{26.5}H_{46}Cl_2CoN_5O_{10}$	$C_{26.5}H_{46}Cl_2FeN_5O_{10}$
M_w	790.30	587.17	724.51	721.43
Space group	$P2_1/n$ (no. 14)	$Pca2_1$ (no. 29)	$P2_1/n$ (no. 14)	$P2_1/n$ (no. 14)
a/Å	12.9270(6)	36.162(2)	17.3793(6)	16.8198(3)
b/Å	17.4997(9)	20.3647(8)	20.9029(6)	21.0452(6)
c/Å	15.2769(9)	11.9060(4)	19.9702(6)	20.6800(6)
β/°	92.95(1)	90	113.35(1)	113.60(1)
V/Å	3451.3(3)	8767.9(7)	6660.6(4)	6708.0(3)
Z	4	12	8	8
T/K	100(2)	100(2)	100(2)	100(2)
D_c/g cm^{-3}	1.521	1.334	1.445	1.429
Diffractometer used	Nonius Kappa-CCD	Nonius Kappa-CCD	Nonius Kappa-CCD	Nonius Kappa-CCD
Refl. collected/$2\theta_{max}$	72291/52.72	55386/60.00	58169/50.00	82667/62.00
Unique refl. ($I > 2\sigma(I)$)	7025/5377	21156/17088	11675/10807	21139/17467
No. of params./restraints	482/186	1045/1	821/1	810/1
μ(Mo-Kα)/cm^{-1}	7.49	7.17	7.35	6.68
$R1$ [a]/goodness of fit [b]	0.0521/1.056	0.0431/1.053	0.0686/1.175	0.0603/1.052
$wR2$ [c] ($I > 2(I)$)	0.1095	0.0768	0.1417	0.1465

[a] Observation criterion: $I > 2\sigma(I)$. $R1 = \Sigma||F_o| - |F_c||/\Sigma|F_o|$. [b] GooF = $[\Sigma[w(F_o^2 - F_c^2)^2]/(n - p)]^{1/2}$. [c] $wR2 = [\Sigma[w(F_o^2 - F_c^2)^2]/\Sigma[w(F_o^2)^2]]^{1/2}$ where $w = 1/\sigma^2(F_o^2) + (aP)^2 + bP$, $P = (F_o^2 + 2F_c^2)/3$.

stirring a methanol solution (5 mL) of tris(2-aminoethyl)amine (0.15 g, 1.0 mmol), solid H[L^{AP}] (0.30 g, 1.0 mmol), and triethylamine (0.28 mL, 2 mmol) at room temperature. The mixture was heated to reflux for 30 min in the presence of air and then cooled to room temperature. After adding a methanol solution (5 mL) of $LiClO_4$ (0.30 g), the dark green solution was allowed to stand under an argon blanketing atmosphere until dark green crystals formed, which were filtered off, washed with cold MeOH, and dried in air. Yield: 0.41 g (68%). ESI-MS: m/z (CH_2Cl_2) = 499 [$(M - ClO_4)^+$, 100%]. Anal. Calc. for $C_{26}H_{43}ClN_5NiO_5$: C, 52.07; H, 7.23; N, 11.86. Found: C, 52.19; H, 7.22; N, 11.56%. Single-crystals of [Ni(tren)(L^{ISQ})]BF_4 have been grown from a CH_3CN solution containing **2** and [(n-Bu)$_4$N]BF_4.

[Co(tren)(L^{ISQ})](ClO_4)$_2$·0.5CH_3OH·0.5H_2O (3). To a solution of $Co(CH_3CO_2)_2$·4H_2O (0.25 g, 1.0 mmol) in MeOH (10 mL) was added with stirring a methanol solution (5 mL) of tris(2-aminoethyl)amine (0.15 g, 1.0 mmol), solid H[L^{AP}] (0.30 g, 1.0 mmol), and triethylamine (0.28 mL, 2.0 mmol) at room temperature. The cobalt was oxidized by a vigorous passage of air through the solution for 3 h. The mixture was heated to reflux for 30 min in the presence of air and then cooled to room temperature. After adding a methanol solution (5 mL) of $LiClO_4$ (0.60 g), the dark brown solution was allowed to stand under an argon blanketing atmosphere until dark brown crystals formed, which were filtered off, washed with cold MeOH, and dried in air. Yield: 0.48 g (66%). ESI-MS: m/z (CH_2Cl_2) = 599 [$(M - ClO_4)^+$, 23%], 250 [$(M - 2ClO_4)^{2+}$, 71%]. Anal. Calc. for $C_{26.5}H_{46}Cl_2CoN_5O_{10}$: C, 43.93; H, 6.40; N, 9.67. Found: C, 43.73; H, 6.32; N, 9.65%.

[Fe(tren)(L^{ISQ})](ClO_4)$_2$·0.5CH_3OH·0.5H_2O (4). To a solution of $FeCl_2$·4H_2O (0.20 g, 1.0 mmol) in MeOH (10 mL) was added with stirring a methanol solution (5 mL) of tris(2-aminoethyl)amine (0.15 g, 1.0 mmol), solid H[L^{AP}] (0.30 g, 1.0 mmol), and triethylamine (0.28 mL, 2.0 mmol) at room temperature. The mixture was heated to reflux for 30 min in the presence of air and then cooled to room temperature. After adding a methanol solution (5 mL) of $LiClO_4$ (0.60 g), the dark blue solution was allowed to stand under an argon blanketing atmosphere until dark blue crystals formed, which were filtered off, washed with cold MeOH, and dried in air. Yield: 0.51 g (71%). ESI-MS: m/z (CH_2Cl_2) = 596 [$(M - ClO_4)^+$, 4%], 248 [$(M - 2ClO_4)^{2+}$, 100%]. Anal. Calc. for $C_{26.5}H_{46}Cl_2FeN_5O_{10}$: C, 44.12; H, 6.43; N, 9.71. Found: C, 44.17; H, 6.36; N, 9.75%.

Physical measurements

Electronic spectra of the complexes and spectra of the spectroelectrochemical investigations were recorded on a HP 8452A diode array spectrophotometer (range: 190–1100 nm). Cyclic voltammograms, square-wave voltammograms, and coulometric experiments were performed using an EG & G potentiostat/galvanostat. Temperature-dependent (2–290 K) magnetization data were recorded on a SQUID magnetometer (MPMS Quantum design) in an external magnetic field of 1.0 T. The experimental susceptibility data were corrected for underlying diamagnetism by the use of tabulated Pascal's constants.

X-Band EPR spectra were recorded on a Bruker ESP 300 spectrometer. The spectra were simulated by iteration of the anisotropic g values, hyperfine coupling constants, and line widths. Zero-field Mössbauer spectra have been recorded by using the equipment described in ref. 3; the programs used for fitting routines have also been described there.

X-Ray crystallographic data collection and refinement of the structures

Dark red and green single crystals of **1** and **2**, respectively, a dark brown crystal of **3** and a dark blue crystal of **4** were coated with perfluoropolyether. Suitable crystals were picked up with a glass fiber and were immediately mounted in the nitrogen cold stream to prevent loss of solvent. Intensity data were collected at 100 K using a Nonius Kappa-CCD diffractometer equipped with a Mo-target rotating-anode X-ray source and a graphite monochromator (Mo-Kα, λ = 0.71073 Å). Final cell constants were obtained from a least squares fit of a subset of several thousand strong reflections. Data collection was performed by hemisphere runs taking frames at 1.0° (**1**, **3**, **4**) or 0.5° (**2**) in ω. Crystal faces of **1** and **2** were determined and the corresponding intensity data were corrected for absorption using the Gaussian-type routine embedded in XPREP [14,15] giving max/min transmission factors of 0.896/0.877 and 0.955/0.808 respectively. Crystallographic data of the compounds are listed in Table 1. The Siemens ShelXTL [14] software package was used for solution and artwork of the structure, ShelXL97 was used for the refinement. The structures were readily solved by direct methods and difference Fourier techniques. All non-hydrogen atoms were refined anisotropically and hydrogen atoms were placed at calculated positions and refined as riding atoms with isotropic displacement parameters. A PF_6^- anion in **1** was found to be disordered over two sites with occupation factors of ~0.7 and 0.3. A split atom model with restrained P–F and

Table 2 Magnetic properties of complexes[a]

Complex	μ_{eff} (290 K)/μ_B	g_{iso}	$\lvert D\rvert$/cm^{-1}	χ_{TIP}/emu mol^{-1}
1	3.1	2.16	3.0 ± 2	165×10^{-6}
2	3.8	2.09 (g_{Ni})	19 ± 5	
		2.0 (g_{rad}) (fixed)		100×10^{-6}
3	1.7	2.0 (fixed)		55×10^{-6} ($\theta = -0.8$ K)

[a] SQUID measurements on powdered samples of complexes in 1.0 T external magnetic field in the temperature range 2–290 K.

Table 3 Electronic spectra of complexes

Complex	Solvent[a]	λ_{max}/nm (ε/M^{-1} cm^{-1})
1	A	300 (5.0×10^3), 390sh, 411 (3.9×10^3), 488 (3.0×10^3)
2	B	307 (7.3×10^3), 360sh, 376 (7.7×10^3), 433 (1.8×10^3), 680sh, 746 (1.6×10^3), 812 (1.4×10^3)
$[Ni^{III}(tren)(L^{IBQ})]^{3+}$ [b]	B	300 (8.0×10^3), 430 (4.2×10^3), 520 (4.1×10^3)
3	A	305 (1.1×10^4), 375 (5.0×10^3), 476 (3.1×10^3), 497 (3.2×10^3), 700sh, 792 (1.1×10^3), 851 (9.8×10^2)
$[Co^{III}(tren)(L^{IBQ})]^{3+}$ [c]	A	320 (8.4×10^3), 480 (4.7×10^3), 590 (1.8×10^3)
$[Co^{III}(tren)(L^{AP}\text{-}H)]^{+}$ [c]	A	305 (9.9×10^3), 360 (8.8×10^3), 710br (1.0×10^3)
4	B	300sh (1.0×10^4), 355 (3.0×10^3), 426 (2.0×10^3), 566sh (4.6×10^3), 654 (6.2×10^3)
$[Fe^{III}(tren)(L^{AP}\text{-}H)]^{+}$ [b]	B	300 (8.6×10^3), 380 (4.2×10^3), 550 (3.0×10^3), 900 (4.0×10^3)

[a] Solvent A: CH_3CN; B: CH_2Cl_2. [b] Electrochemically generated in CH_2Cl_2 (0.10 M $[N(n\text{-}Bu)_4]PF_6$). [c] Electrochemically generated in CH_3CN (0.10 M $[N(n\text{-}Bu)_4]PF_6$).

F–F distances was introduced applying SADI-instructions.[15] The structure analysis of **2** revealed that the asymmetric unit contains three crystallographically independent molecules of which two are related by a pseudo-translation parallel to the *a* axis. Split models were also used to account for the disorder of a methanol molecule of crystallization in isostructural **3** and **4**.

CCDC reference numbers 197833–197836.

See http://www.rsc.org/suppdata/dt/b2/b211698g/ for crystallographic data in CIF or other electronic format.

Results and discussion

1 Synthesis of complexes

The reaction of one equivalent of tris(2-aminoethyl)amine, and 1 equiv. of 2-anilino-4,6-di-*tert*-butylphenol with $Ni(CH_3CO_2)_2{\cdot}4H_2O$, $Co(CH_3CO_2)_2{\cdot}4H_2O$, or $FeCl_2{\cdot}4H_2O$ in methanol solution containing 2 equiv. of NEt_3 in the presence of oxygen affords the mononuclear complexes $[Ni(tren)(L^{IBQ})](PF_6)_2$ (red–black) (**1**), $[Ni(tren)(L^{ISQ})](ClO_4)$ (dark-green) (**2**), $[Co^{III}(tren)(L^{ISQ})](ClO_4)_2{\cdot}0.5CH_3OH{\cdot}0.5H_2O$ (brown) (**3**), and $[Fe^{III}(tren)(L^{ISQ})](ClO_4)_2{\cdot}0.5CH_3OH{\cdot}0.5H_2O$ (blue) (**4**) in good yields after addition of $LiPF_6$ or $LiClO_4$. Slow recrystallization of the crude products from CH_3OH solutions yielded single crystals suitable for X-ray crystallography.

For the synthesis of **1** a vigorous stream of air was passed through the reaction vessel at ambient temperature whereas **2** was generated by heating the reaction mixture to reflux for 30 min in the presence of air but without passing fresh air through the solution.

The electronic structure of complexes and evaluation of the oxidation level of the *O*,*N*-coordinated ligands as $(L^{ISQ})^{1-\bullet}$ or $(L^{IBQ})^0$ has been achieved by temperature dependent magnetic susceptibility measurements and recording of their electronic spectra. Table 2 summarizes the magnetic properties and Table 3 gives electronic spectra of complexes **1**–**4**.

Fig. 1 displays the temperature dependence of the magnetic moments of complexes **1**–**3**. Complex **1** possesses an $S = 1$ ground state typical for octahedral Ni(II) (d^8). This renders the *o*-aminophenol derived bidentate ligand an *o*-iminobenzoquinone since it must be neutral and diamagnetic. Thus **1** should be described as $[Ni^{II}(tren)(L^{IBQ})]^{2+}$ which is the first example for a stable *O*,*N*-coordinated *o*-iminobenzoquinone.

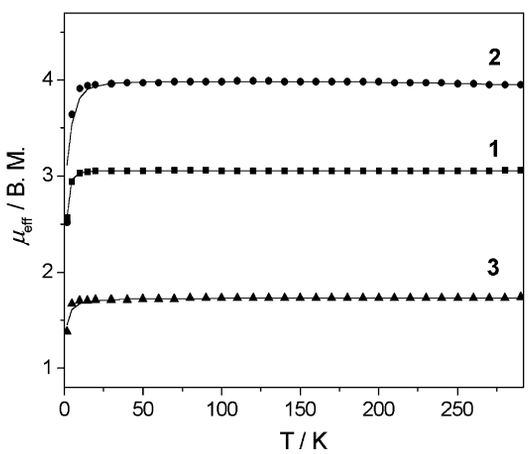

Fig. 1 Temperature dependence of the effective magnetic moment, μ_{eff}, of complexes **1**, **2** and **3**. Solid lines represent best fits by using parameters given in Table 2 and the text.

Interestingly, complex **2** possesses an $S = 3/2$ ground state which is attained *via* strong intramolecular ferromagnetic coupling between a nickel(II) ion ($S_{Ni} = 1$) and an *o*-iminobenzosemiquinonate(1−) π radical ($S_{rad} = {}^1/_2$). The solid line in Fig. 1 represents a best fit using the spin Hamiltonian $H = -2JS_{Ni}{\cdot}S_{rad}$ with parameters $J = 200$ (± 10) cm^{-1}, $g_{Ni} = 2.09$, $g_{rad} = 2.0$ (fixed) and a zero-field splitting $|D|_{3/2} = 19 \pm 5$ cm^{-1}. Similar behavior has been reported for other octahedral Ni(II) complexes containing coordinated organic π radicals.[10,11,16] The d_{z^2} and $d_{x^2-y^2}$ magnetic orbitals (σ-symmetry) of the nickel ions and the ligand π orbital containing the unpaired radical electron are strictly orthogonal in this octahedral complex and the intramolecular spin exchange coupling is therefore ferromagnetic in nature.

Complex **3** displays a temperature-independent magnetic moment of 1.7 μ_B indicating the presence of an *O*,*N*-coordinated radical anion, $(L^{ISQ})^{1-\bullet}$, with an $S_{rad} = ½$ ground state ($g_{rad} = 2.000$ (fixed), $\chi_{TIP} = 55 \times 10^{-6}$ emu mol^{-1}; $\theta = -0.79$ K) and a diamagnetic cobalt(III) ion (d^6, $S_{Co} = 0$).

Complex **4** is diamagnetic, $S = 0$, in the temperature range 4–300 K.

The presence of *O*,*N*-coordinated ligands $(L^{AP}\text{-}H)^{2-}$, $(L^{ISQ})^{1-\bullet}$ or $(L^{IBQ})^0$ in a given coordination compound has been

shown previously[2] to give rise to a series of very intense intraligand transitions in the UV and visible region. Table 3 summarizes the spectra and Fig. 2 shows the spectra of **1**, **2**, Fig. 3 that of **3** and Fig. 4 that of **4**. These absorption bands are fairly diagnostic for the oxidation level of the *o*-aminophenol derivative present since d–d transitions are much weaker and tren is colorless. Most characteristically the M(L^{ISQ}) fragment displays three broad, intense ($\varepsilon \sim 10^3$ M^{-1} cm^{-1}) absorption maxima in the range 600–1000 nm which are absent in M(L^{IBQ}) or M(L^{AP}-H) species. For M(L^{IBQ}) fragments two maxima at ~400 and ~480 nm ($\varepsilon > 1.5 \times 10^3$) are typical.[2] Therefore, the spectrum of **1** clearly indicates the presence of an Ni(L^{IBQ}) moiety whereas in **2**, **3** and **4** the corresponding M(L^{ISQ}) fragment is observable.

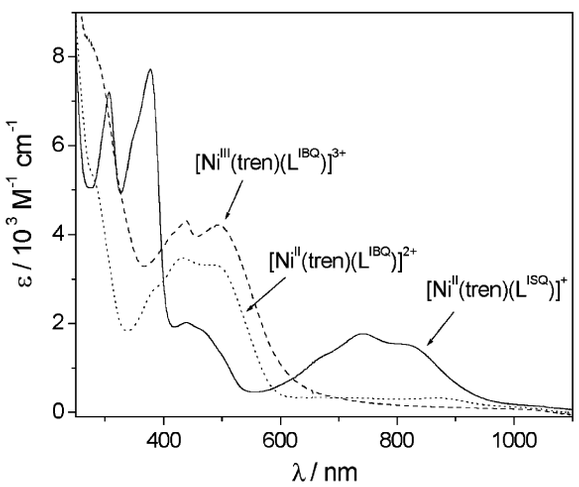

Fig. 2 Electronic spectra of **2** in CH_2Cl_2, its electrochemically one-electron oxidized form $[Ni^{II}(tren)(L^{IBQ})]^{2+}$ and its two-electron oxidized form $[Ni^{III}(tren)(L^{IBQ})]^{3+}$.

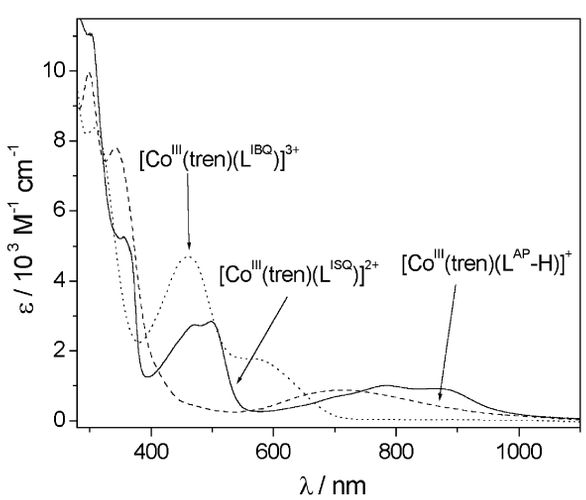

Fig. 3 Electronic spectra of **3** in CH_3CN, its electrochemically generated one-electron oxidized form $[Co^{III}(tren)(L^{IBQ})]^{3+}$ and its one-electron reduced form $[Co^{III}(tren)(L^{AP}\text{-H})]^{+}$.

2 Crystal structures

The crystal structures of complexes **1**–**4** have been determined by X-ray crystallography at 100(2) K. Crystallographic data are given in Table 1; Table 4 summarizes some important bond distances. All compounds contain an octahedral cation [M(tren)(L^{IBQ} or L^{ISQ})]$^{n+}$ with a tetradentate tren ligand and either an *O*,*N*-coordinated *o*-iminobenzoquinone, $(L^{IBQ})^0$, or an *o*-iminobenzosemiquinonate(1−) π radical anion. The structure of the monocation $[Ni^{II}(tren)(L^{ISQ})]^+$ in crystals of **2** is shown in Fig. 5; those of the cations in crystals of **1**, **3** and **4** are similar and not shown.

Table 4 Selected bond distances (Å) for the cations in crystals of **1**–**4**

	1 (M = Ni)	**2**[a] (M = Ni)	**3**[a] (M = Co)	**4**[a] (M = Fe)
M–N7	2.054(3)	2.033(2)	1.921(3)	1.859(2)
M–N30	2.072(3)	2.106(2)	1.964(3)	2.009(2)
M–N36	2.074(3)	2.149(2)	1.956(3)	2.007(2)
M–N39	2.111(3)	2.133(2)	1.955(3)	2.007(2)
M–O1	2.119(2)	2.053(2)	1.885(3)	1.910(2)
M–N33	2.128(3)	2.096(2)	1.971(4)	2.012(2)
O1–C1	1.234(4)	1.294(3)	1.323(5)	1.296(2)
C1–C2	1.463(4)	1.435(3)	1.418(6)	1.431(3)
C1–C6	1.519(4)	1.465(3)	1.436(6)	1.442(3)
C2–C3	1.349(5)	1.374(3)	1.376(6)	1.373(3)
C3–C4	1.467(4)	1.427(3)	1.430(6)	1.443(3)
C4–C5	1.352(4)	1.370(3)	1.367(6)	1.371(3)
C5–C6	1.432(4)	1.430(3)	1.421(6)	1.425(3)
C6–N7	1.301(4)	1.348(3)	1.349(5)	1.345(2)
C8–N7	1.435(4)	1.421(3)	1.425(5)	1.436(3)

The numbering scheme is as in Fig. 5. [a] Data are given for a single independent cation only.

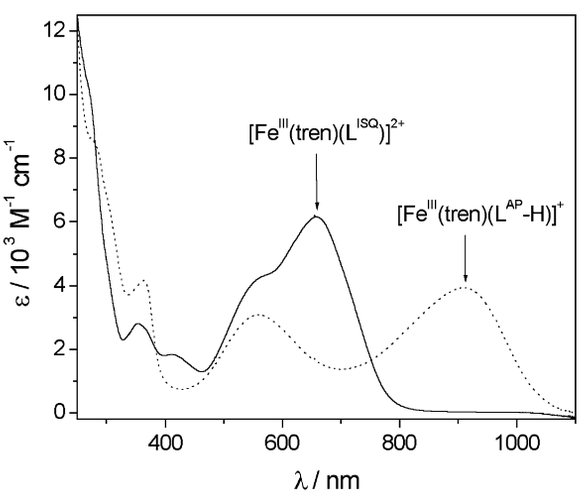

Fig. 4 Electronic spectra of **4** in CH_2Cl_2 and its electrochemically generated one-electron reduced form $[Fe^{III}(tren)(L^{AP}\text{-H})]^{+}$.

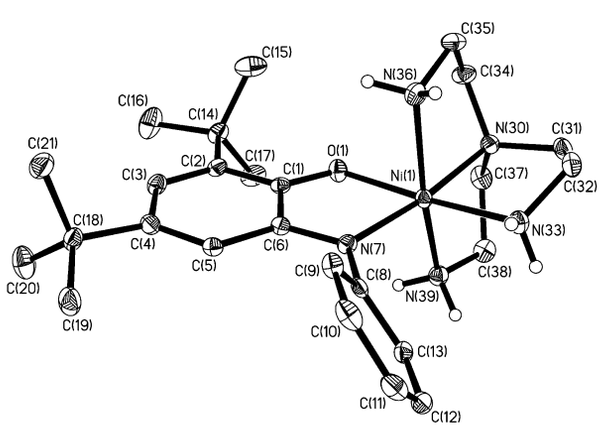

Fig. 5 Structure of the monocation $[Ni^{II}(tren)(L^{ISQ})]^+$ in crystals of **2**. Those of the dications in crystals of **1**, **3** and **4** are similar and not shown. The amine hydrogen atoms are shown as small open circles; all other H-atoms are omitted for clarity.

Scheme 1 gives average C–O, C–N and C–C bond lengths of *O*,*N*-coordinated ligands $(L^{AP}\text{-H})^{2-}$, $(L^{ISQ})^{1-\bullet}$ and $(L^{IBQ})^0$. As expected, the C–O and C–N bonds of the aminophenol derived six-membered rings shrink with increasing level of oxidation of these ligands; they are very short in $(L^{IBQ})^0$, intermediate in the π radical $(L^{ISQ})^{1-\bullet}$ and rather long (single bonds) in the aromatic ligand $(L^{AP}\text{-H})^{2-}$. In addition, the six C–C bonds

Table 5 Redox potentials[a] of complexes

Complex	$E^1_{1/2}$[b]/V	$E^2_{1/2}$[b]/V	$E^3_{1/2}$[b]/V
1, **2**	0.97 r.	−0.36 r.	−1.28 r.
3	0.27 r.	−0.58 r.	−1.36 (irr.)[c]
4	0.67	−0.52	−1.33 (irr.)[c]

[a] *Conditions*: CH_2Cl_2 solution (0.10 M $[(n\text{-}Bu)_4N]PF_6$; glassy carbon working electrode; scan rate 100 mV s^{-1}; ferrocene (Fc) internal standard). [b] Referenced *vs.* the Fc^+/Fc couple. [c] Peak potential $E_{p,red}$/V; r = reversible, irr = irreversible.

of the six-membered ring are nearly equidistant within the 3σ level in $(L^{AP}\text{-}H)^{2-}$ but show a quinoid-type distortion in the radical $(L^{ISQ})^{1-\bullet}$ and a true quinone structure in $(L^{IBQ})^0$ with two alternating C=C double bonds at 1.36 Å and four longer single bonds. Thus, the crystal structure determinations unambiguously demonstrate the presence of a $(L^{ISQ})^{1-\bullet}$ ligand in **2**, **3** and **4**, respectively, but an $(L^{IBQ})^0$ in **1**. Complex **1** represents the first structurally characterized coordination compound with an *O*,*N*-coordinated *o*-iminobenzoquinone ligand.

Furthermore, the M–O and M–N bond lengths in the above complexes **1** and **2** are typical for octahedral Ni(II) ions (d^8, $S = 1$) and for low-spin cobalt(III) (d^6) in **3**, and low-spin ferric ion (d^5, $S_{Fe} = ½$) in **4**.[7] The diamagnetic ground state of **4** is then readily explained *via* strong intramolecular antiferromagnetic exchange coupling between a t_{2g}^5 configurated ferric ion and a π radical anion $(L^{ISQ})^{1-\bullet}$. A series of such complexes has been reported recently.[7] Similarly, for $[Cr^{III}(tren)(3,6\text{-}DTBSQ)](PF_6)_2$ a temperature-independent magnetic moment of 2.85 + 0.10 μ_B ($S = 1$) has been reported indicating a strong antiferromagnetic coupling between the Cr(III) (d^3; t_{2g}^3) ion and the semiquinonate radical anion.[13]

3 Spectro- and electro-chemistry

Fig. 6 displays the cyclic voltammograms (CV) of complexes **2**, **3** and **4** in CH_2Cl_2 solution (0.10 M $[(n\text{-}Bu)_4N]PF_6$) recorded at a glassy carbon working electrode. Table 5 gives the redox potentials referenced *versus* the ferrocenium–ferrocene, Fc^+/Fc, couple.

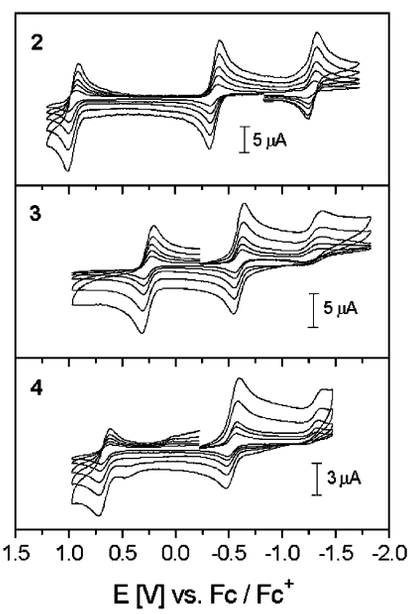

Fig. 6 Cyclic voltammograms of **2**, **3** and **4** at 20 °C in CH_2Cl_2 solution (0.10 M $[(n\text{-}Bu)_4N]PF_6$ supporting electrolyte; glassy carbon working electrode; scan rates 25, 50, 100, 200 and 400 mV s^{-1}, ferrocene internal standard).

The CV exhibits three reversible one-electron transfer waves of which two at 0.92 and −0.36 V *vs.* Fc^+/Fc correspond to one-electron oxidations whereas the process at −1.28 V corresponds to a reversible one-electron reduction of **2**. Scheme 2 summarizes these transfers and distinguishes between ligand and metal-centered processes. Thus the monocation $[Ni^{II}(tren)(L^{ISQ})]^+$ undergoes a reversible ligand-centered oxidation generating the dication $[Ni^{II}(tren)(L^{IBQ})]^{2+}$ and it may be reduced (also ligand-centered) yielding $[Ni^{II}(tren)(L^{AP}\text{-}H)]^0$. Interestingly, the oxidation of the dication is metal-centered yielding an octahedral, tricationic Ni^{III} species $[Ni^{III}(tren)(L^{IBQ})]^{3+}$. These assignments are corroborated by coulometry of **2** at appropriately fixed potentials and spectroelectrochemical measurements. Fig. 2 shows the electronic spectra of the tri-, di- and mono-cation where clearly both the tri- and the di-cation exhibit the spectral features of the $(L^{IBQ})^0$ ligand whereas the monocation has those of an $(L^{ISQ})^{1-\bullet}$ ligand. The solution of the neutral species $[Ni^{II}(tren)(L^{AP}\text{-}H)]^0$ is not stable enough (very O_2 sensitive) to allow its spectrum to be recorded.

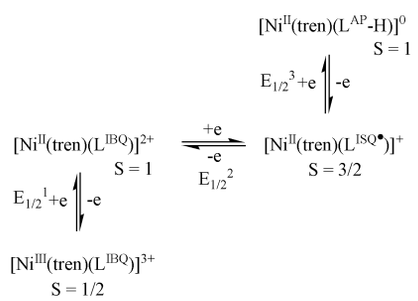

Scheme 2

The cyclic voltammogram of **3** (Fig. 6) exhibits two reversible and a quasi-reversible one-electron transfer waves which correspond to i) a ligand-centered oxidation of **3** yielding $[Co^{III}(tren)(L^{IBQ})]^{3+}$ at E = 0.27 V and ii) a reduction generating $[Co^{III}(tren)(L^{AP}\text{-}H)]^+$ at −0.58 V and, finally, iii) a metal-centered, ill-defined reduction $Co^{III} \longrightarrow Co^{II}$ at E = −1.36 V. The spectra of these tri-, di- and monocations are shown in Fig. 3. The presence of the $(L^{IBQ})^0$ ligand in the trication and of $(L^{ISQ})^{1-\bullet}$ in the dication is clearly established. The monocation displays a weak transition of a Co^{III} ion at 710 nm which could be a metal-to-ligand charge transfer band.

The CV of **4** (Fig. 6) displays a reversible one-electron oxidation at 0.67 V *vs.* Fc^+/Fc and a reversible one-electron reduction at −0.52 V *vs.* Fc^+/Fc which correspond to ligand-centered processes shown in eqn. (1).

$$[Fe^{III}(tren)(L^{IBQ})]^{3+} \underset{+e}{\overset{-e}{\rightleftharpoons}} [Fe^{III}(tren)(L^{ISQ})]^{2+} \underset{+e}{\overset{-e}{\rightleftharpoons}} [Fe^{III}(tren)(L^{AP}\text{-}H)]^{1+} \quad (1)$$

$S = ½$ $\qquad$ $S = 0$ $\qquad$ $S = ½$

Fig. 4 shows the spectra of the di- and mono-cation; the presence of $(L^{ISQ})^{1-\bullet}$ in **4** is clearly seen whereas for its one-electron reduced form the two maxima at 550 and 900 nm are assigned to ligand $(L^{AP}\text{-}H)^{2-}$-to-metal charge transfer bands.

The zero-field Mössbauer spectrum of the dication has been recorded. Complex **4** exhibits a single quadrupole doublet with an isomer shift of 0.25 mm s^{-1} and a quadrupole splitting of 2.07 mm s^{-1} at 80 K. These data are very similar to those reported for three complexes $[cis\text{-}(cyclam)Fe^{III}(L^{\bullet})](PF_6)_2$ where $(L^{\bullet})^{1-}$ represents three differently substituted *o*-iminobenzosemiquinonate(1−) π radicals and cyclam is 1,4,8,11-tetraazacyclotetradecane.[7] As pointed out there the data support the assignment of a low spin ferric electron configuration ($S_{Fe} = ½$).

4 X-band EPR Spectra

Fig. 7 shows the X-band EPR spectrum of **2** in frozen CH_2Cl_2 solution (0.10 M $[(n\text{-}Bu)_4N]PF_6$) at 10 K and its simulation. Clearly, an $S = 3/2$ signal is observed with $|D|_{3/2} = 10 \pm 5$ cm^{-1}, $E/D = 0.21$, $g_x = 2.10$, $g_y = 2.10$, $g_z = 2.06$ in accord with the susceptibility measurements reported above. Thus the monocation $[Ni^{II}(tren)(L^{ISQ})]^+$ possesses an $S = 3/2$ ground state which is attained *via* strong ferromagnetic coupling between an octahedral Ni(II) ion, $S_{Ni} = 1$, and an $(L^{ISQ})^{1-}$ radical anion, $S_{rad} = ½$. In contrast, the trication which is the two-electron oxidized form of **2** exhibits the X-band EPR spectrum at 10 K shown in Fig. 8 which consists of two $S = ½$ signals. The electrochemically generated trication is not quite stable and decomposes slowly generating an organic uncoordinated π radical with $g_{iso} = 2.005$. The low spin Ni(III) species $[Ni^{III}(tren)(L^{IBQ})]^{3+}$ possesses an $S = ½$ ground state with $g_x = 2.17$, $g_y = 2.15$ and $g_z = 2.04$.

The X-band spectrum of **3** in CH_2Cl_2 solution at 298 K shown in Fig. 9 confirms the $S = ½$ ground state of the dication $[Co^{III}(tren)(L^{ISQ})]^{2+}$. From a simulation the following parameters have been obtained: $g = 1.997$, $A(^{59}Co) = 14.0$ G, $A(^{14}N) = 8.8$ G, line width = 5.5 G. The observed ^{59}Co hyperfine coupling is very similar to data reported for Co^{III}(benzosemiquinonate) complexes.[17] Note that coupling to only one nitrogen of the radical ligand is observed.

Finally, the X-band EPR spectrum of the electrochemically one-electron reduced form of **4** in CH_2Cl_2 (0.10 M $[(n\text{-}Bu)_4N]PF_6$) shown in Fig. 10 clearly establishes an $S_{Fe} = ½$ ground state of the monocation $[Fe^{III}(tren)(L^{AP}\text{-}H)]^+$. The established g values at $g_x = 2.159$, $g_y = 2.131$, $g_z = 1.946$ are in excellent agreement with a low spin ferric configuration and does not correspond to a ligand radical in the redox isomer $[Fe^{II}(tren)(L^{ISQ})]^+$ containing a low spin ferrous ion although it is noted that the g-anisotropy is quite small and contributions from an Fe(II)–semiquinone form cannot be completely ruled out.

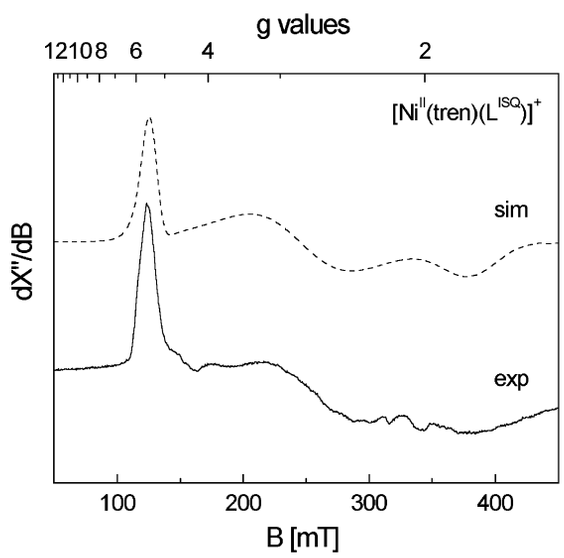

Fig. 7 X-Band EPR spectrum of **2** in frozen CH_2Cl_2 solution at 10 K (conditions: frequency 9.6384 GHz, modulation amplitude 10 G, power 2.0 μW).

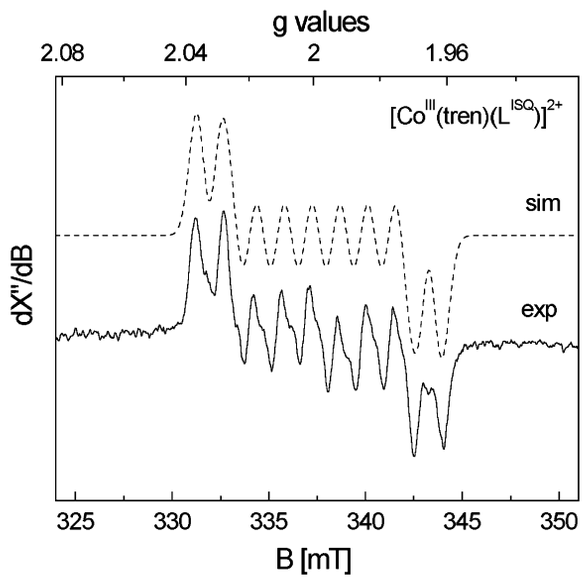

Fig. 9 X-Band EPR spectrum of **3** in CH_2Cl_2 solution at 298 K (conditions: frequency 9.44215 GHz, modulation amplitude 2.0 G, power 0.016 μW).

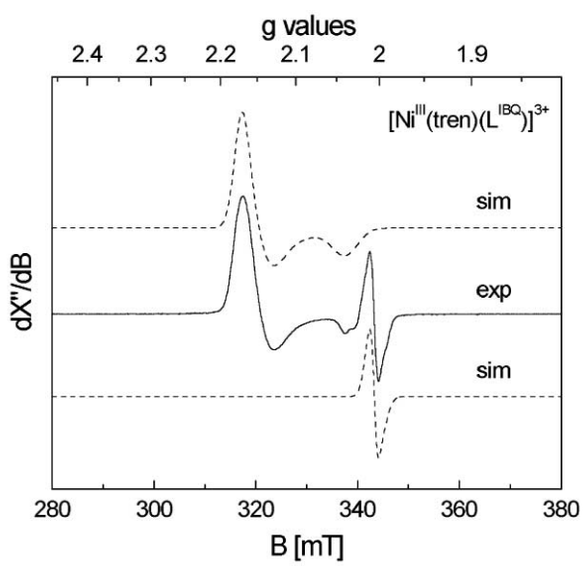

Fig. 8 X-Band EPR spectrum of electrochemically generated $[Ni^{III}(tren)(L^{IBQ})]^{3+}$ in frozen CH_2Cl_2 (0.10 M $[(n\text{-}Bu)_4N]PF_6$) at 10 K (conditions: frequency 9.6379 GHz, modulation amplitude 10 G, power 0.064 μW).

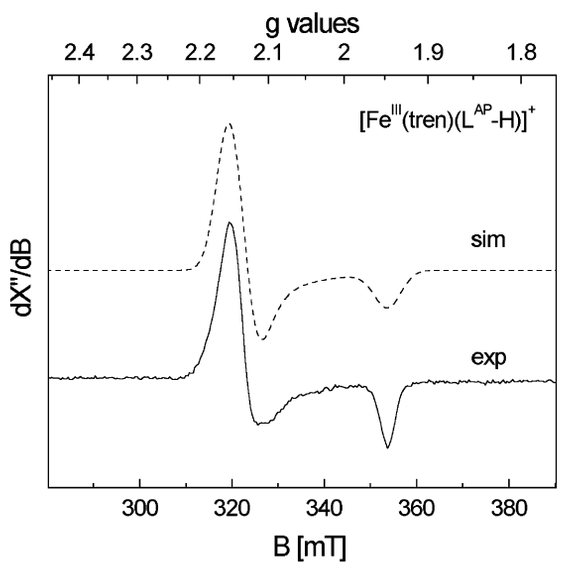

Fig. 10 X-Band EPR spectrum of electrochemically generated one-electron reduced form of **4** in CH_2Cl_2 solution (0.10 M $[(n\text{-}Bu)_4N]PF_6$) (conditions: frequency 9.6382 GHz, modulation amplitude 10 G, power 0.010 μW).

Conclusions

The most salient features of this study are:

1. The geometrical details of the diamagnetic, *O*,*N*-coordinated *o*-iminobenzoquinone ligand have been established in **1** for the first time by X-ray crystallography. The C=O and C=N distances are short and indicate double bond character. The six-membered ring clearly displays quinone character with two alternating short C=C double bonds and four longer C–C bonds.

2. The corresponding *O*,*N*-coordinated *o*-iminobenzosemiquinonate(1−) π radical anion is present in **2**, **3** and **4**. The metrical details differ from those of *O*,*N*-coordinated (L^{IBQ}), $(L^{AP}\text{-}H)^{2-}$ or $(L^{AP})^{1-}$ (Scheme 1). The spin exchange coupling of the π radical $(L^{ISQ})^{1-\bullet}$ with the $d_{x^2-y^2}$, d_{z^2} magnetic orbitals of octahedral Ni^{II} is *ferromagnetic* in **2** (S_t = 3/2) but *antiferromagnetic* with half-filled d_{xy}, d_{xz}, d_{yz} magnetic orbitals, *e.g.* **4**.

3. Thus, complex **4** contains a low spin ferric ion (d^5, $S_{Fe} = ½$) which couples strongly *antiferromagnetically* to the π radical anion yielding a diamagnetic ground state ($S_t = 0$).

Acknowledgements

K. S. M. thanks the Max-Planck-Society for a fellowship. We are grateful to the Fonds der Chemischen Industrie for financial support.

References

1 C. N. Verani, S. Gallert, E. Bill, T. Weyhermüller, K. Wieghardt and P. Chaudhuri, *Chem. Commun.*, 1999, 1747.
2 P. Chaudhuri, C. N. Verani, E. Bill, E. Bothe, T. Weyhermüller and K. Wieghardt, *J. Am. Chem. Soc.*, 2001, **123**, 2213.
3 H. Chun, C. N. Verani, P. Chaudhuri, E. Bothe, E. Bill, T. Weyhermüller and K. Wieghardt, *Inorg. Chem.*, 2001, **40**, 4157.
4 H. Chun, T. Weyhermüller, E. Bill and K. Wieghardt, *Angew. Chem., Int. Ed.*, 2001, **40**, 2489.
5 H. Chun, P. Chaudhuri, T. Weyhermüller and K. Wieghardt, *Inorg. Chem.*, 2002, **41**, 790.
6 X. Sun, H. Chun, K. Hildenbrand, E. Bothe, T. Weyhermüller, F. Neese and K. Wieghardt, *Inorg. Chem.*, 2002, **41**, 4295.
7 H. Chun, E. Bill, E. Bothe, T. Weyhermüller and K. Wieghardt, *Inorg. Chem.*, 2002, **41**, 5091.
8 V. Bachler, G. Olbrich, F. Neese and K. Wieghardt, *Inorg. Chem.*, 2002, **41**, 4179.
9 (*a*) L. C. G. Vasconcellos, C. P. Olveira, E. E. Castellano, J. Ellena and I. S. Moreira, *Polyhedron*, 2000, **20**, 493; (*b*) G. Speier, J. Csihony, A. M. Whalen and C. G. Pierpont, *Inorg. Chim. Acta*, 1996, **245**, 1–5.
10 C. G. Pierpont and C. W. Lange, *Prog. Inorg. Chem.*, 1994, **41**, 331.
11 C. G. Pierpont and A. S. Attia, *Collect. Czech. Chem. Commun.*, 2001, **66**, 33.
12 P. A. Wicklund and D. G. Brown, *Inorg. Chem.*, 1976, **15**, 396.
13 D. E. Wheeler and J. K. McCusker, *Inorg. Chem.*, 1998, **37**, 2296.
14 ShelXTL V.5, Siemens Analytical X-Ray Instruments, Inc., 1994.
15 ShelXL97, G. M. Sheldrick, Universität Göttingen, 1997.
16 (*a*) T. M. Barclay, R. G. Hicks, M. T. Lemaire and L. K. Thompson, *Chem. Commun.*, 2000, 2141; (*b*) T. M. Barclay, R. G. Hicks, M. T. Lemaire and L. K. Thompson, *Inorg. Chem.*, 2001, **40**, 5581; (*c*) T. M. Barclay, R. G. Hicks, M. T. Lemaire, L. K. Thompson and Z. Xu, *Chem. Commun.*, 2002, 1688; (*d*) R. G. Hicks, M. T. Lemaire, L. K. Thompson and T. M. Barclay, *J. Am. Chem. Soc.*, 2000, **122**, 8077.
17 (*a*) P. A. Wicklund, L. S. Beckmann and D. G. Brown, *Inorg. Chem.*, 1976, **15**, 1996; (*b*) R. M. Buchanan and C. G. Pierpont, *J. Am. Chem. Soc.*, 1980, **102**, 4951; (*c*) S. L. Kessel, R. M. Emberson, P. G. Debrunner and D. N. Hendrickson, *Inorg. Chem.*, 1980, **19**, 1170.